Fabrication and Electrochemical Characterization of PEDOT:PSS based electrodes

---

Bachelor Thesis

Johannes Kepler University Linz, Austria

INSTITUTE OF PHYSICAL CHEMISTRY AND LINZ INSTITUTE FOR ORGANIC SOLAR CELLS

Beatrice Hurbean

Supervisor: Manuela Schiek, apl.-Prof.Dr.

Abstract

Poly(3,4-ethylenedioxythiophene):poly-(styrene sulfonate) (PEDOT:PSS) has been one of the most studied organic semiconductors in the recent years and the electrochemical characterization of the compound was the focal point of this thesis. A specific PH1000 solution mix from *Otgonbayar Erdene-Ochir* Master thesis "*Investigation of Polymer Electrode – Electrolyte Interfaces for Future Neurostimulating Photosensors"* was used as a basis of these experiments and slight additive variations of the recipe were analyzed and compared. Additionally, two different filters, polytetrafluorethylene (PTFE), and regenerated cellulose (RC), were used to investigate the hydrophobic effect of the PTFE filter on the hydrophilic PH1000 solution. Single layers of the PH1000 solution and double layers, comprised of a Clevios™ CPP 105D (CPP) layer and PH1000 layer, were spin coated on glass and indium tin oxide (ITO) in order to analyze conductivity, film thickness, appliance, and electrical conductivity.

The experiments of this thesis have shown an improvement of appliance with the use of the PTFE filters while the conductivity was wildly varying, and the electrical capacitance was barely present. The RC filtered samples had an improved conductivity and electrical capacitance when compared to the PTFE results, but the solutions were not reliably coating an even layer on either glass or ITO.

Double layered samples have shown improvements in the coating process of PH1000 for both PTFE and RC filtered solutions and a decrease in conductivity and electrical capacitance due to the nature of CPP layer.

The additives dodecylbenzene sulfonic acid (DBSA) and dimethyl sulfoxide (DMSO) had no significant differences but the percentage change between 1 and 2% of the (3-glycidyloxypropyl)trimethoxysilane (GOPS) additive has shown that samples which contained GOPS 1% were performing better overall.

Table of Contents

1. Introduction

1.1 Retinitis pigmentosa

Retinitis pigmentosa (=RP) is an overarching term for diseases which affect the layer of photoreceptors located in the eye retina. It causes degradation of vision over several decades until photoreceptor apoptosis (cell death) occurs in the affected retinal cells. The disease is classified as a genetic disorder since it is only acquired hereditarily but it is not confined to one inheritance mode. World-wide there are roughly 1.5 million people affected by RP causing retinal degeneration for 1 in 3 000 to 1 in 5 000 people. [1], [2]

The affected photoreceptors are special cells divided into two types, rods, and cones. Each of these cells are distributed differently throughout the retina and perform different functions. Rod cells are increasingly more present towards the sides of the retina since they are responsible for night-time vision (scotopic vision) and peripheral vision. Contrary to the rods, the cones are overwhelmingly present in the center and evenly distributed amongst the rods throughout the rest of the retina. The cone cells are responsible for day-time vision (photopic vision) due to their structure which allows for color perception and a high visual acuity in well luminated conditions. In general, photoreceptor cells convert a specific light range into signals which can be biologically processed by nerve cells. This mechanism, also known as phototransduction, is possible due to special proteins called opsins which are within the photoreceptors and absorb photons that can cause a change in the cell's membrane potential. The number of photons necessary for a change in the membrane potential varies between rods and cones.
While rod and cone cells are one of the most important cell types in the retina there are a variety of other cell structures which work together to receive and process the visual information. After the rods and cones layer there are horizontal cells, bipolar cells, amacrine cells and ganglion cells. [3-7]

The first symptom which is noticed in individuals affected by RP is the slow progressive loss of scotopic vision and peripheral vision. The rod cells are the first cell type to reach cell apoptosis since they secrete a neuroprotective substance to protect cones from undergoing degradation first. After the rod cells are lost, the cone photoreceptors degradation can no longer be delayed, and the cone degeneration can result in complete blindness in certain individuals. How far the

photoreceptors degrade is dependable on the gene mutations which are responsible for the coding of the RP. Currently it is estimated that there are 300 genes which could carry a mutation linked to RP. [7], [8-10]

1.2 PEDOT:PSS organic semiconductor

There are a variety of scientific research fields which search for better conducting polymers such as organic solar cells, fuel cells, thermoelectrical devices, optoelectronics, and many more. Currently the most widely used and analyzed polymer within these fields is an organic semiconductor known as poly(3,4-ethylenedioxythiophene):poly(styrene sulfonate) (PEDOT:PSS). This polymer solution is composed of two ionomers which are molecules that repeatedly switch between electrically neutral compounds and ionized compounds. Additionally, the different ionomer units are covalently bonded to a polymer chain which creates the backbone of the molecule structure with the ionomers being the pendant group moieties. [11], [12]

For example, the PSS structure is a sulfonated polystyrene derived from sodium polystyrene sulfonate. The sulfonyl groups are negatively charged in a tandem pattern which fits the ionomer pattern of the PEDOT compound when they are synthesized into PEDOT:PSS. Attached to the backbone polymer chain polystyrene (PS) is the pendant group moiety as seen in Figure 1.

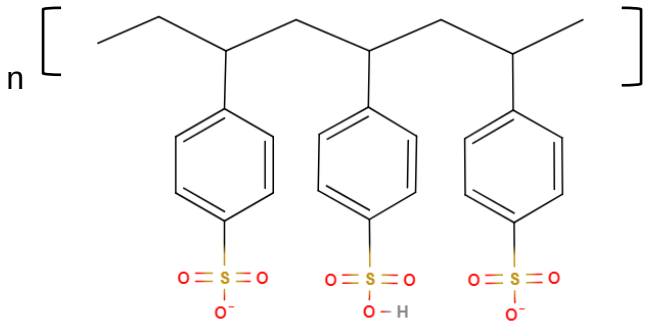

Figure 1. Molecular structure of sulfonated polystyrene with alternating deprotonated sulfonyl groups

The production of PEDOT:PSS starts by using an aqueous solution containing PSS and 3,4-ethylenedioxythiophene (EDOT) monomers. By oxidizing the EDOT monomer into a radical $[EDOT]^+$ via sodium persulfate ($Na_2S_2O_8$) it can then react with another neutral EDOT to form the PEDOT polymer with the counter ions from the PSS. [13]

After the production of the PEDOT:PSS polymers the morphology of the compound aggregates to PEDOT-rich areas and PSS-rich areas. The PEDOT-cores, which are highly conductive, are

surrounded by excess PSS chains that offer the necessary counter ions. These counter ions are necessary to maintain neutrality in the PEDOT structure so that oxidation and reduction can be induced to the PEDOT molecules. The interaction between the PEDOT polymer chain and PSS can be seen in Figure 2. [11]

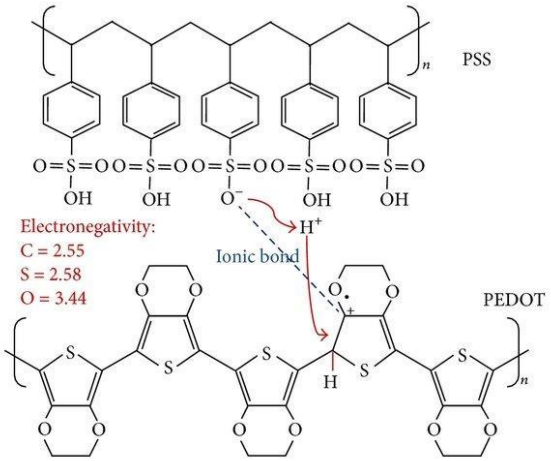

Figure 2. Reaction between PEDOT and PSS structure, adapted from [11]

The PEDOT polymer is a conjugated molecule which means that the π-orbitals contain delocalized electrons that can move within the structure. This delocalization of electrons within the PEDOT material is one of the reasons why PEDOT:PSS is favored as an organic semi-conductive polymer. Many conductive materials, such as Ag/AgCl are often times too reactive to be used for bioelectrical purposes, but PEDOT:PSS allows for both a conductive, flexible, and biocompatible compound which can be cheaply manufactured.

Many experiments aiming at analyzing the electrochemical properties of PEDOT:PSS are done via cyclic voltammetry (CV), an electrochemical method used to induce oxidation and reduction states of a material in a repeating pattern. The cyclic voltammetry reaction for compounds which have π-conjugated orbitals such as PEDOT can be described as such. [11], [14]

$$PEDOT^0 + A^+PSS^- \rightarrow PEDOT^+PSS^- + A^+ + e^-$$

The A^+ in this reaction is an ion within the electrolyte solution and PEDOT is being oxidized while the PSS works as a negative counter ion. This reaction is often very visible during cyclic voltammetry. When PEDOT:PSS is coated on a material it is generally seen as a transparent or light blue layer, but when oxidized the color changes to an intense deep blue hue. Once the

oxidation process is complete the color remains until the CV starts the reduction sweep. The deep blue color dissipates, indicating the gain of electrons within the PEDOT structure. For many conductive compounds, the oxidation and reduction reaction are correlated with the electrical capacitance of the material. [15]

The PEDOT:PSS material is very ductile and flexible allowing the polymer to be applied to a wide range of structures that are either rigid like indium tin oxide (ITO) or bendable such as polyethylene terephthalate (PET). While it has many advantages, there are still improvements which are necessary to make PEDOT:PSS a commercial replacement for materials such as ITO that have been a staple in the production of solar cells, light emitting diodes and transparent electrodes. [12]

1.2.2 Modifications and improvements

The versatility and usage of PEDOT:PSS is still being improved and researched since the solution requires additives to support the shortcomings of the compound. Some of the disadvantages of PEDOT:PSS solutions are the very high surface tension which can make spin-coating a film challenging. Additionally, when PEDOT:PSS films are produced for bioelectronic purposes, dissolution and delamination is observed due to the PSS-rich areas having a high solubility in water and other polar solvents.

Current improvements of PEDOT:PSS stability in water is via the additive of a crosslinker known as (3-glycidyloxypropyl)trimethoxysilane (GOPS). The GOPS molecule binds to available PSS-nucleophiles which lowers the PSS-rich areas solubility in aqueous solutions and the available counter ions. An illustration of the crosslinked structure of PEDOT:PSS can be seen in Figure 3. [14], [16], [17]

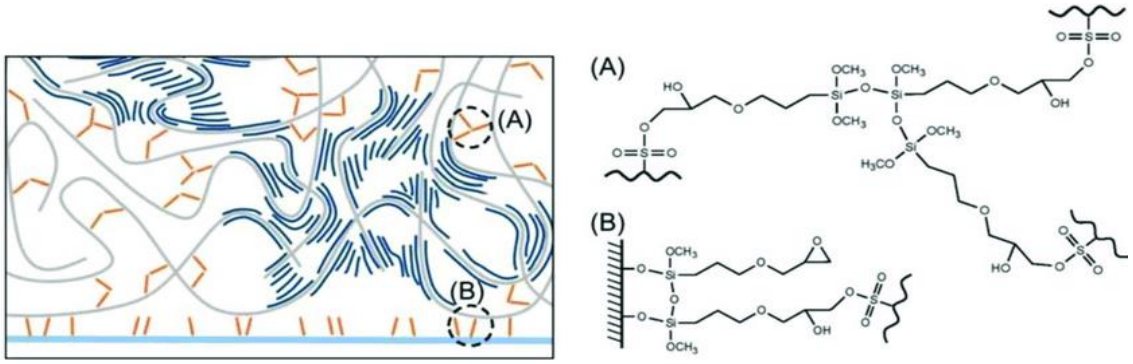

Figure 3. PEDOT-cores (blue) with PSS-rich areas (gray) containing GOPS (yellow) which binds to free PSS-nucleophiles producing PSS-GOPS, GOPS-GOPS (A) and GOPS-glass (B bonds), adapted from [18]

Furthermore, DBSA is used as a surfactant and its conductivity enhancement is still being investigated, while DMSO is widely used as a PEDOT:PSS additive for increased conductivity. The DMSO additive has a higher affinity to water thus increasing electron-phonon coupling and improving the carrier density of PEDOT:PSS. Other compounds which are used to improve conductivity are glycerol, sorbitol, and ethylene glycol (EG). [19-21]

1.3 ITO

A commonly used transparent semiconductor is indium tin oxide (ITO). The material consists of a lattice made out of mixed oxides of indium and tin (see Figure 4).

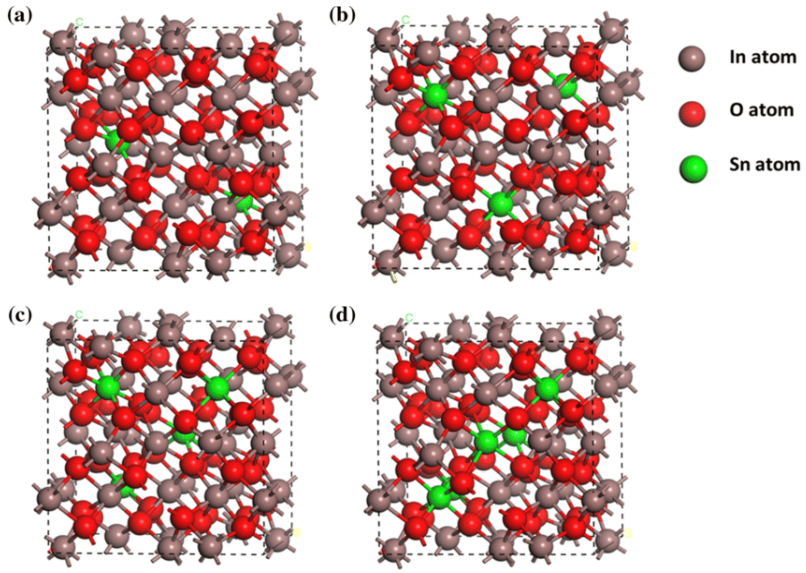

Figure 4. ITO structure with different ratios of tin to indium oxide, (a) In_2O_3-2Sn, (b) In_2O_3-3Sn, (c) In_2O_3-4Sn. (d) In_2O_3-5Sn, adapted from [22]

It is applied in many areas such as plasma displays, touch panels, polymer-based electronics, thin film photovoltaics and in optoelectronics. While ITO can be coated on a variety of materials, it is expensive to produce, and the film has a lower flexibility with increasing conductivity. There are many alternative materials which are being researched due to the high cost and rigidity of ITO. Graphene, for example, is a carbon-based semiconductor which is a flexible material with high transparency. Furthermore, PEDOT:PSS is also analyzed as a conductive polymer which, due to its flexibility, could potentially replace ITO. A variety of research produced on PEDOT:PSS investigates additives for the polymer which can improve shortcomings such as an overall lower conductivity when compared to inorganic materials. [23-27]

2. Aim

This research aims at improving and analyzing PEDOT:PSS based electrodes in Krebs-Ringer HEPES electrolyte such that the electrode would be stable and functional within a cell environment and thus possibly applicable to retinal implants. The capacity and stability of ITO under oxygen is additionally analyzed via cyclic voltammetry to test whether ITO glass would be a compatible coating basis for the PEDOT:PSS electrode. The PEDOT:PSS coatings are tested for conductivity, appliance, and electrical capacitance with varying methods.

The objective of this work was achieved by:

- Using preexisting PEDOT:PSS based electrode protocols from *Otgonbayar Erdene-Ochir* [28] and exchanging DBSA for DMSO to improve conductivity
    - Conductivity is tested by applying PEDOT:PSS on glass and using van-der-Pauw method and profilometer

- Analyzing the transmission of PEDOT:PSS on glass which was done by apl.-Prof.Dr. Manuela Schiek

- Testing different GOPS concentrations (1-2%) to improve appliance of PEDOT:PSS as well as testing different filters such as RC and PTFE

- Analyzing ITO in a Krebs-Ringer electrolyte under oxygen to test for the electrode's oxidation range in cyclic voltammetry

- Analyzing PEDOT:PSS based electrodes capacitance on ITO via cyclic voltammetry

3. Materials and Methods

3.1 Materials

Special materials such as Clevios™ PEDOT:PSS PH1000 solution were obtained from Heraeus Electronic Materials. The Clevios™ CPP 105D was acquired from the same company but the solution is no longer being manufactured and thus an older CPP solution, which was in storage since March 2019, was used for this project.
Furthermore, the mixture which was used as a GOPS crosslinker was Silquest A-187 from the manufacturer Momentive Performance Materials Inc.

3.2 Solution compositions

There were two solution variations with either a CPP or PH1000 basis, which were prepared based on the research done by Otgonbayar Erdene-Ochir in "Investigation of Polymer Electrode – Electrolyte Interfaces for Future Neurostimulating Photosensors". These mixtures were used to create coats on standard glass and ITO coated glass. Additionally, a Ringer-Krebs solution was prepared for cyclic voltammetry measurements. [28]

3.2.1 Preparation of coating solutions

First, the formula for the mixture using CPP as a basis was unaltered and is described in Table 1.

Table 1.: Formula for CPP solution, adapted from [28]

Component	Volume (µl)	Percent (%)
CPP	5000	93
Glycerol	269	5
GOPS	107.5	2

The glycerol (Sigma-Aldrich) was used to enhance the morphology of the CPP mixture and the GOPS acted as a crosslinker between the two substances. [28]

Next, solutions containing PH1000 were varied. During the experiments, four different PH1000 solutions were tested. The first two solution compositions contained DBSA (Fluka), which was later switched out for DMSO (Sigma-Aldrich), and each of the mixtures had a varied GOPS

concentration (between 1-2%). Tables 2.1 through Tables 2.4 describe the compositions of the four different PH1000 solutions.

Table 2.1: PH1000 mixture containing DBSA and GOPS 1%, adapted from [28]

Component	Volume (µl)	Percent (%)
PH1000	5000	93.5
Glycerol	267	5
GOPS	53.5	1
DBSA	26.7	0.5
Total	5347.2	100

Table 2.2: PH1000 mixture containing DBSA and GOPS 2%, adapted from [28]

Component	Volume (µl)	Percent (%)
PH1000	5000	92.5
Glycerol	270.2	5
GOPS	108.1	2
DBSA	27	0.5
Total	5405.3	100

Table 2.3: PH1000 mixture containing DMSO and GOPS 1%

Component	Volume (µl)	Percent (%)
PH1000	5057.50	89
Glycerol	284.1	5
GOPS	56.82	1
DMSO	284.1	5
Total	5682.52	100

Table 2.4: PH1000 mixture containing DMSO and GOPS 2%

Component	Volume (µl)	Percent (%)
PH1000	5000.75	88
Glycerol	284.1	5
GOPS	113.64	2
DMSO	284.1	5
Total	5682.59	100

All the solutions were mixed in a 10 mL glass vial and stirred for two days at room temperature. The CPP based mixtures can be stored in the fridge after stirring while the PH1000 solutions needed to be filtered. The filtration of the solutions was either done via PTFE (pores, 0.45 µl) (Sigma-Aldrich) or RC filters (pores, 0.45 µl) (Minisart® Sartoriust). Once the process is completed, the mixtures can be stored in the fridge for seven days in prime condition and a maximum of fourteen days after which the solution quality will significantly deteriorate.

3.2.2 Preparation of electrolyte solution

The cyclic voltammetry experiments required a buffer solution which could simulate the extracellular environment of a cell. For this purpose, a Ringer-Krebs solution buffered with HEPES was composed as described in Table 3 for 1 L. The pH of the mixture was adjusted to be 7.4 by addition of a NaOH solution with a concentration of 1 mol/L. [28]

Table 3: Composition of Ringer-Krebs buffer with HEPES for 1 L, adapted from [28]

Components	m (g)	M (g/mol)	c (mmol/L)
Sodium chloride (NaCl)	8.1816	58.4400	140.0
Potassium chloride (KCl)	0.3728	74.5513	5.0
Magnesium chloride ($MgCl_2$)	0.0952	95.2110	1.0
Calcium chloride ($CaCl_2$)	0.2220	110.9900	2.0
D-(+)-Glucose	1.8016	180.1560	10.0
HEPES	2.3830	238.3012	10.0

The chemicals $MgCl_2$, $CaCl_2$, D-(+)-Glucose and HEPES were obtained from Sigma-Aldrich. NaCl was procured from Herba Chemosan Apotheker-AG and KCl from Alfa Aesar.
The components were first dissolved in a beaker containing approximately 900 mL of deionized water. Afterwards, the pH of the solution was adjusted with NaOH and tested with a pH-electrode until it reached 7.4 pH. The 900 mL were then decanted in a 1 L volumetric flask which was then filled up with 100 mL of deionized water.

3.3 Sample coating

Several different coatings were tested during this project as well as different combinations of coatings. There were single coatings of either CPP or PH1000 solutions and combined coatings with the first layer being the CPP mixture and the second layer being a PH1000 mixture. The materials used as a coating basis were either glass, for conductivity measurements, or ITO for CV measurements.

3.3.1 Spin coating

The vast majority of layers were coated for 60 seconds at 1500 rpm and an acceleration of 1500 (rpm/sec), with the exception of the CPP layer which had two variants. If the CPP solution was spin coated with the above-mentioned parameters, it was denoted as CPP (slow) and the second variant, denoted as CPP (fast), was spin coated for 60 seconds at 2000 rpm and an acceleration of 2000 (rpm/sec). The differentiation of CPP (slow) and CPP (fast) was only used for ITO samples, while all layers for the glass samples were spin coated with the slower setting.
The annealing temperature was a constant 140°C for all mixtures while the annealing time for the layers depended on the solution which was used. The CPP coating would be heated for 15 minutes on a heating plate (Präzitherm), and PH1000 layers would be left for 1 hour. If the sample consisted of a double layer, first CPP and subsequently PH1000, then the sample would need 5-10 minutes to cool off between the first annealing and the second coating process.

3.3.2 Glass sample coating

Glass samples were used for measuring sheet resistances (=R_s) and cut from 76 x 25 x 1 mm microscopic slides (Marienfeld). The samples were cut to be 25 x 25 mm^2 in size and properly cleaned before use. The cleaning process was done manually but an ultrasonic bath could also be used instead.
The glass was first wiped with a tissue soaked in acetone, after which it was dried, and then cleaned a second time with deionized water. Excess water was removed with a new tissue and any remaining dust was blown off with N_2 gas. This process was repeated until there were no visible stains or dust particles on the glass. The amount of solution which was needed for spin coating varied between the CPP solution and the PH1000 solution. Since CPP would more easily adhere to the glass, 350 µl of the solution would suffice by placing it in the center of the sample. PH1000 could also be spin coated with the same process and volume, but the success rate of the PH1000 mixture forming an even layer under such conditions was much lower than for CPP due to the solution's lack of adhesive properties to the glass. To increase the probability of an even PH1000 layer it is recommended to use ~650 µl and coat the entire surface with the solution before spin coating. The samples were spin coated as described in section 3.3.1 (see above) and stored in a plastic box containing six wells.

3.3.3 ITO sample coating

ITO glass was chosen as the base material for the cyclic voltammetry measurements. Since the CV experiments required a long rectangular glass (see CV section 3.6), the overall dimensions of the ITO glass were cut to be a minimum of 10 x 50 mm or a maximum of 10 x 60 mm.
The dimensions were not the standard sample form for spin coating purposes. The total width of 10 mm was the smallest size which the spin coater could pull a vacuum on, and the longitudinal design of the glass was not the ideal form to use for spin coating. This resulted in the following modifications.

The cut ITO was placed next to a ruler and a double-sided tape, which did not leave residual glue, was used to tape off the section that would not be spin coated and submerged into the CV cell solution. The untapped side should measure exactly 10 x 30 mm and the tapped side could vary depending on the overall cut of the sample length.
As previously mentioned, the samples can be cleaned via ultrasonic bath which should be done before the ITO is taped, but all cleaning processes in these experiments were performed manually.
In order to clean the ITO glass, a tissue soaked with acetone is used to remove any visible stains from the glass. Subsequently, the sample is washed with acetone and the excess solution is removed with N_2 gas.
Deionized water can also be used to further clean the glass, but it should not be the last step before spin coating the ITO sample. Since the excess water needs to be removed with a tissue, undetectable residue from the tissue can be left on the glass which can interfere with the spin coating. Due to acetones quick evaporation with the use of N_2 gas, the contact of the ITO glass with other materials can be kept at a minimum if it is washed with acetone before coating.
Once the cleaning process is completed, the ITO needs to be placed off center on the spin coater as it is portrayed in Figure 6.

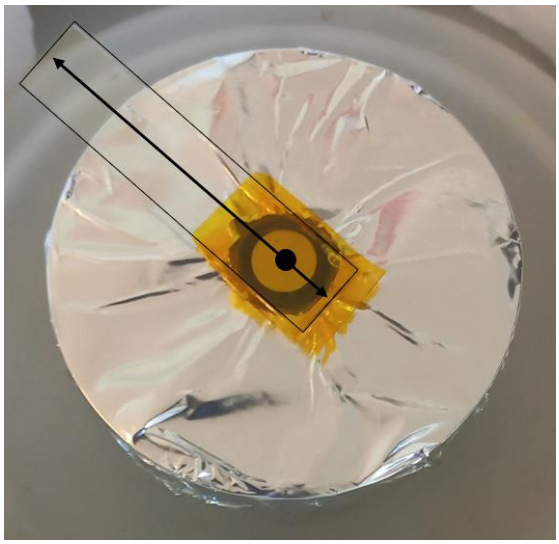

Figure 6.: ITO sample placed on the spin coater off-center to ensure that the untapped area is coated more effectively. The arrows portray the force which is applied to the solution during spin coating from the center of rotation

With an off-center placement of the sample, it is important to test the stability of the glass on the spin coater before the solution is applied. ITO glass with a maximum length of 60 mm should not be placed at the very edge of the tapped half, since the imbalance will cause the sample to fall off. The right placement of such samples can be approximated by placing the tapped side such that the center of the tapped area is on the vacuum opening of the spin coater. This will provide sufficient counterweight for the sample to be spin coated at a maximum of 2000 rpm. Any parameters higher than 2000 rpm will not hold the sample on the spin coater under these arrangements.

If the stability of the ITO glass on the spin coater was tested, then the mixture can be applied to the uncoated area.

For ITO samples it is important to always coat the entire area since the solution will not be pushed out evenly in all directions (see Figure 6). Approximately +120 µl was used for both CPP and PH1000 mixtures for coating the area. It should be noted that the PH1000 solutions have a high surface tension which could result in more volume being needed if the solution is not applied to the edges of the glass first and then to the center. Once the entire area is coated, the spin coating process is completed as described in section 3.3.1. The samples were stored in a plastic box with no wells.

3.4 Four-point probe [29]

The sheet resistance of CPP and PH1000 layers was measured via the four-point probe van der Pauw method. In general, van der Pauw utilizes four electrodes which are applied to the corner points of a sample. Due to the placement of the probes being nonlinear, the resulting sheet resistance is thus an overall average of the material.

The samples in this experiment were tested with a Keithley 2400 SourceMeter. The corners of the coated glass samples were first covered by a thin layer of liquid conductive silver to enhance the contact sensitivity between the probe and the tested material. The liquid silver was applied with the use of a toothpick to ensure that the layer of the silver would not be exceedingly thick. After the silver had dried, the probes were placed on the glass and connected to the machine as described in Figure 7.

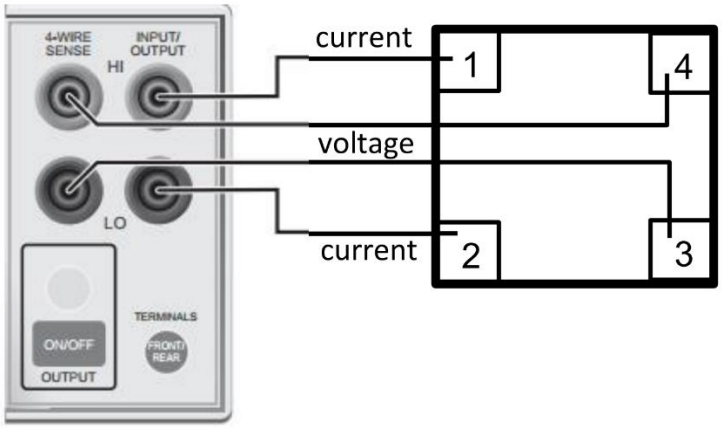

Figure 7. A counterclockwise placement of the probes on a sample and the wire connection to the Keithley 2400 machine, adapted from [29]

The machine sources current from two probes to the opposing electrodes which would measure the voltage drop across the film. For example, the above Figure 7 sources a current to probe ½ and measures the vertical voltage drop across the film with probe 4/3. There were four configurations, two vertical and two horizontal measurements, for each sample to calculate a more accurate R_s (see Table 4).

Table 4. Wire configurations of four measurements, two vertical and two horizontal, adapted from [29]

	Device Contact Position			
Front Panel Wire Position	**Vertical 1**	**Vertical 2**	**Horizontal 1**	**Horizontal 2**
Output Hi	1	4	1	2
Output Lo	2	3	4	3
Sense Hi	4	1	2	1
Sense Lo	3	2	3	4

Once the average $R_{vertical}$ and $R_{horizontal}$ are evaluated, the sheet resistance can be calculated via the van der Pauw equation (eq. 1) and the resistivity can then be obtained by additionally measuring the film thickness (eq. 2). [29]

$$e^{\frac{-\pi R_{vertical}}{R_s}} + e^{\frac{-\pi R_{horizontal}}{R_s}} = 1 \qquad \text{(eq. 1)}$$

.

3.5 Profilometer

The layer thickness of the samples was tested with a stylus profilometer (Dektak XT, Bruker). Each sample had four measuring lines which were obtained by scratching the annealed layer(s) off with a needle without damaging the glass underneath. The four lines were placed such that the measurements would show the different film thickness at the top, center, and bottom of the sample. An average was then calculated from the four data points. Finally, with the measured R_s and film thickness of a sample, the resistance and conductivity of the layer(s) could be calculated with the following equations:

Equation for resistivity (eq. 2):

$$\rho = R_s \cdot t \qquad \text{(eq. 2)}$$

ρ … resistivity

R_s … sheet resistance

t … film thickness

The equation for conductivity is the inverse of resistivity (eq. 3):

$$\sigma = \frac{1}{\rho} \qquad \text{(eq. 3)}$$

σ … conductance

ρ … resistivity

3.6 Cyclic voltammetry

The CV experiments use a standard three-electrode configuration. A Ag/ AgCl electrode in a 3 M KCl solution was used as a reference electrode and for the counter electrode a platinum wire was utilized. The coated ITO samples were then applied as a working electrode and the electrodes were connected to an Invium Vertex One potentiostat. All measurements were recorded with the software IviumSoft.

The platinum wire was cleaned before every experiment by heating it up with a Bunsen burner for approximately one minute.

3.6.1 Electrochemical cell and CV parameters

For the electrochemical cell a 10 mL vial (VWR) was used, and the top of the plastic cap (VWR) was cut out and replaced by a circular rubber pad.

One hole was punched out of the pad for the reference electrode, and a straight line of approximately 12 mm was cut through the top such that the 10 mm wide ITO samples could be pushed through.

The vial was first filled with roughly 9 mL electrolyte solution (see section 3.2.2) and the counter electrode was threaded through the rubber with a hollow needle (Henke-Sass, Wolf GMBH). Subsequently, the tape from the ITO sample was removed and the sample was pushed through the rubber from the bottom of the cap starting from the uncoated part of the ITO. The cap was screwed onto the vial once the coated side of the ITO was below the pad and the uncoated side above. The reference electrode, Ag/ AgCl electrode, was carefully pushed into the hole without disturbing the counter or working electrode. The individual electrodes should not be in contact with one another, and the working electrode was placed deeper into the electrolyte than the counter electrode. Figure 8 depicts a complete setup of the electrochemical cell.

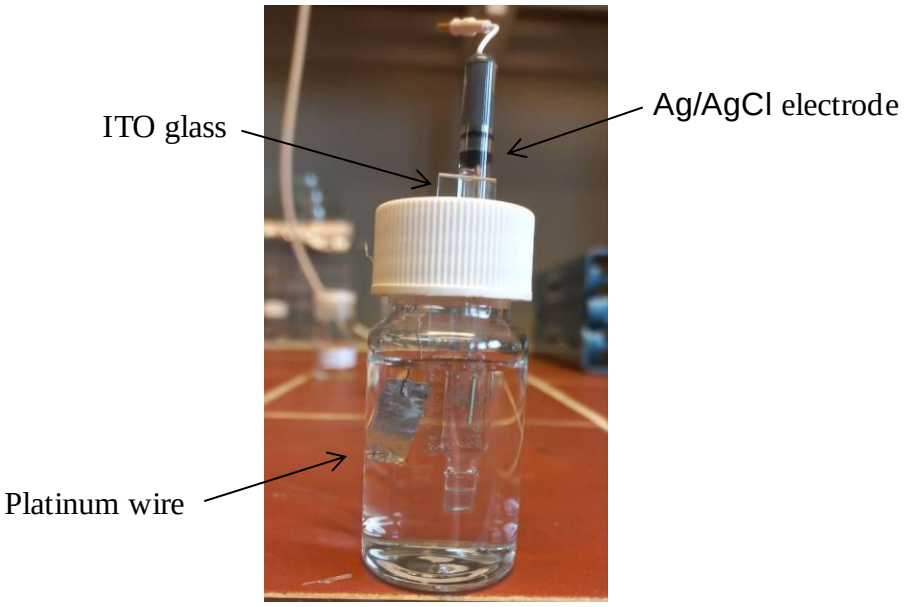

Figure 8. Electrochemical cell setup with platinum wire (=counter electrode), ITO sample (=working electrode), Ag/AgCl electrode in 3 M KCl solution (reference electrode)

Once the electrochemical cell was ready and properly connected to the Ivium Vertex One potentiostat, the following parameters for uncoated ITO glass were set as can be seen in Table 5.

Table 5. CV settings for uncoated ITO glass

Parameter	Value
Cycles	4-5
E steps	10 mV
Vertex 1	0.8 V
Vertex 2	-1.5 V
Scan rate	50 mV/s

All cyclic voltammetry experiments were first swept in the positive direction until the first vertex followed by a negative sweep to the negative value for vertex 2 and a final positive sweep towards the origin. Many of these parameters were unmodified for the single layered and double layered PH1000 samples with the exception of Vertex 2 which was -1 V, and the scan rate. The settings for the scan rate were changed with varying increments starting at 200 mV/s then 150, 100, 50, 30, 20 and finally 10 mV/s. The samples were not moved or touched between the change of each scan rate and the analysis was done subsequently. After the 10 mV/s scan, the ITO glass of the samples was oxidized for the purpose of measuring the submerged area size. This oxidation was achieved by letting the CV run with the above-mentioned parameters in Table 5.

4. Results and Discussion

In order to determine which PH1000 solution provided the best improvement in terms of conductivity, appliance, transmission, and electrical capacitance several sample groups were constructed and analyzed.
The three major distinguishing factors were, used filter (PTFE or RC), PH1000 mixture additive (DBSA/ DMSO) and GOPS concentration (1 or 2%). Then, further separations were constructed between samples which had a single coating of either CPP or PH1000 mixture and samples which had a double coating of CPP and PH1000 layers.

ITO glass was used as the basis for the PEDOT:PSS electrodes and thus the working potential range of the ITO electrode needed to be established before any CV experiments could be performed for the PEDOT:PSS electrodes. Furthermore, the ITO was tested under oxygen and nitrogen conditions since the entire electrode structure with the PH1000 coating would have to work under the presence of oxygen. The nitrogen experiments were performed to create a better analysis of the results from the CV experiments since it would eliminate any recordings of reduction and oxidation peaks of oxygen reactions which could overlap with the ITO oxidation.

4.1 Cyclic voltammetry of bare ITO

The CV experiments for ITO were first done under oxygen and then performed under nitrogen gas with the previously mentioned parameters in section 3.6.1. The first experiments conducted under oxygen conditions caused the ITO to oxidize which was apparent due to the color change of the glass. The previously transparent glass would appear with a bronze shimmering layer after the CV analysis and the color would become increasingly more intense with each cycle.

The reduction and oxidation peaks were visible on the graph, but it was not clear whether the recorded peaks were from the oxygen reaction or from the ITO as can be seen in Figure 9.

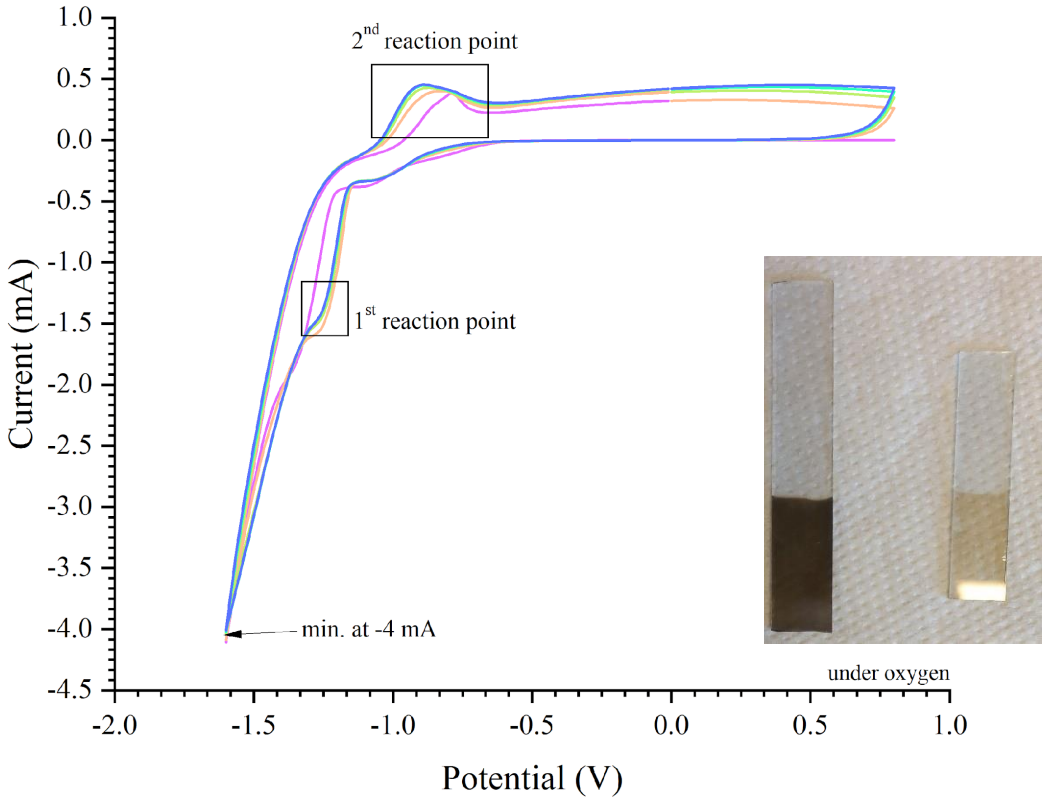

Figure 9. CV graph of an ITO glass sample under oxygen conditions showing two defined reaction points and the physical appearance of the reaction on the ITO glass

The first reduction curve which can be seen in Figure 9 is around the potential of -1.4 V and the second reaction peak starts at -1 V and ends at approximately -0.7 V. The ITO glass would start to become discolored after the first peak at -0.8 V which would indicate that the two recorded reaction points would be of the reduction and oxidation of ITO. The most probable product of ITO oxidation was In_2O_3, but the experiment needed to be performed under nitrogen to draw any clear conclusions. The discoloration of the ITO would range between a light ochre to an intense dark brown color which always had a metallic reflection. The intensity of the color would change depending on how much ITO was exposed during the CV and how many cycles were performed on the sample. This led to the conclusion that the discoloration of the ITO was linked with either a byproduct which was produced during the reduction reaction or the oxidation product In_2O_3.

The next Figure 10 shows the ITO cyclic voltammetry under nitrogen conditions and the graph no longer depicts the first reduction curve that can be seen in the previous experiment under oxygen. There are no clear reactions during the negative sweep for the CV under nitrogen.

Instead of the first reduction curve, a flat line is visible followed by the hydrogen evolution reaction (HER) which commonly occurs in cyclic voltammetry experiments at approximately -1.0 V.

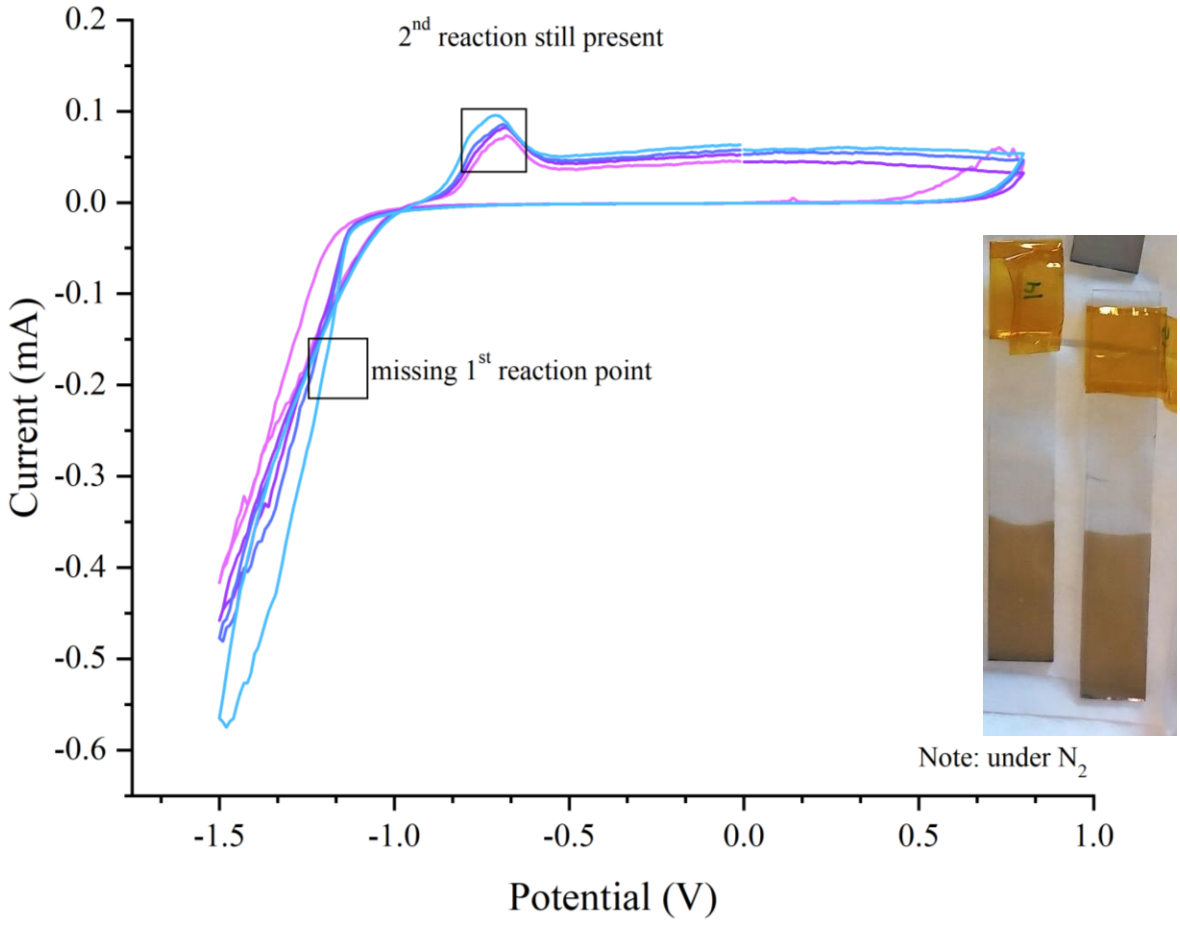

Figure 10. CV of ITO under nitrogen which is missing the first reduction curve seen for CV if ITO under oxygen and the physical effects of the reduction and oxidation on the ITO glass

This experiment shows that the first reaction curve at -1.4 V from the oxygen CV was the reduction of O_2 instead of ITO. The ITO reduction curve happens earlier at approximately -1.1 V right before the hydrogen evolution reaction. The oxidation curve at -0.8 V is still present in the CV under nitrogen conditions thus affirming that the peak is the oxidation of ITO. Further experiments were done with ITO under nitrogen, but the vertex 2 parameter would be changed from -1.5 V to -1 V which was slightly before the ITO reduction curve. The ITO glass would not become discolored as shown by the samples in Figure 10 and 11.

This led to the following conclusions and comparisons between the CV tests under oxygen and nitrogen conditions which can be seen in Figure 11.

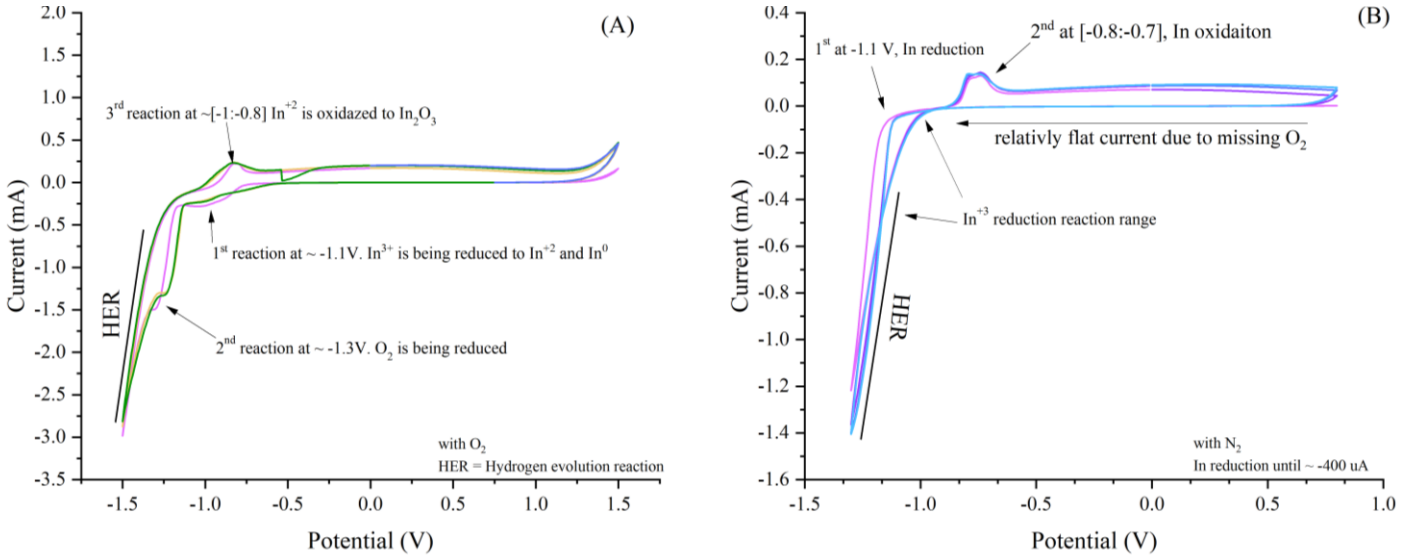

Figure 11. The left graph (A) depicts CV of ITO with oxygen and the right graph (B) depicts CV of ITO with nitrogen

The ITO glass starts to reduce from In^{3+} to In^{+1} and In^{0} at -1.1 V and then In^{+1} oxidizes at -0.8 V to In_2O_3 even without the presence of O_2 in the electrolyte. This was concluded when the oxidation peaks from the different CVs were compared. The peak for ITO samples under O_2 would be in the range of 0.3 and 0.4 mA while ITO under N_2 conditions would generally be below 0.1 mA. Since In_2O_3 formed even without a surplus of O_2 it led to the conclusion that In^{0} was also being produced for the purpose of releasing oxygen for the formation of In_2O_3 from In^{+1}. This oxidation does not occur if the In is not fully reduced from its In^{3+} state, which was observable from the CV that only ran until the vertex 2 point -1 V. The ITO CV with the vertex 2 at -1 V had a current above -400 µA and the glass did not become discolored which was a visual sign that the ITO glass oxidized to In_2O_3. This leads to the conclusion that the In reduction reaction range is from -1 V to -1.1 V and the recorded current range is approximately from -0.95 µA to -410 µA.

The cyclic voltammetry experiments for PH1000 samples were thus conducted only until the vertex 2 point of -1 V so that a clear graph of the reduction and oxidation of PEDOT:PSS could be seen without the ITO reaction.

4.2 PTFE filtered solutions and samples

One of the biggest issues encountered during these experiments was the appliance of the PH1000 mixtures on both glass and ITO. The high surface tension of the PEDOT:PSS solutions made it difficult to achieve an even coating across the desired area of the sample. One possible improvement was to create a CPP film first which would allow for a better and more even coating of the PH1000 mixtures at the expense of the overall conductivity and transmission.
Experiments from Otgonbayar Erdene-Ochir have also reported delamination issues for the PH1000 solutions. [28] In the search for a better adhesive and stable PH1000 mixture the standard RC filter was changed for PTFE to observe the effects of a hydrophobic filter on a hydrophilic solution. Furthermore, the DBSA was replaced by DMSO to possibly improve conductivity of the PH1000 solution.

4.2.1 Appliance and conductivity on glass samples (PTFE)

Filtering the PH1000 solutions, regardless of the additives DBSA/ DMSO and GOPS concentration, proved problematic. The PTFE filter heavily resisted filtering the solution and a lot of force needed to be applied but the yielded PH1000 mixture had a smaller surface tension and a highly improved appliance to the glass samples. Spin-coating without a CPP film was far more successful than previously and an even coating covering the full area of the sample was achieved on ITO as well.
Once the appliance was improved successfully, the conductivity of the samples needed to be tested and compared.
The measured sheet resistance varied for each sample with highly different standard deviations and a summary can be seen in Table 6.

Table 6. Average sheet resistance of single layer PH1000 and double layer CPP/ PH1000 with additives DBSA, DMSO and GOPS 1 or 2 %, the sample amount (with removed outliers) and the standard deviation

Coating	Sample Nr	Avg. sheet resistance (Ω)	St. dev (+/-)
PH1000/ DBSA/ GOPS 1%	2	197	43
PH1000/ DBSA/ GOPS 2% *	1	188	/
CPP/ PH1000/ DBSA/ GOPS 1%	2	195	15
CPP/ PH1000/ DBSA/ GOPS 2%	3	236	45
PH1000/ DMSO/ GOPS 1% *	1	166	/
PH1000/ DMSO/ GOPS 2% *	1	217	/
CPP/ PH1000/ DMSO/ GOPS 1%	3	181	29
CPP/ PH1000/ DMSO/ GOPS 2%	3	286	89

The sheet resistance standard deviation was far higher for samples containing 2% GOPS concentration. This could indicate that the cross-linking and entanglement properties of GOPS become more unpredictable and uneven throughout the solution the higher the concentration was. In some cases such as PH1000/ DBSA/ GOPS 2% and PH1000/ DMSO/ GOPS 2% the sheet resistance was so vastly different that many of the samples were considered outliers and could not be taken into account for the final data (marked with *).

Samples containing GOPS 2% could have a sheet resistance ranging from 194 Ω to 512 Ω regardless of double layer or single layer.

The different effects between the DBSA and DMSO additive was not very apparent from the sheet resistance data, thus the transmission values which were provided by apl.-Prof.Dr. Manuela Schiek were used to get a better comparison. The sheet resistance of the samples was plotted against the transmission data at 550 nm as can be seen in Figure 12.

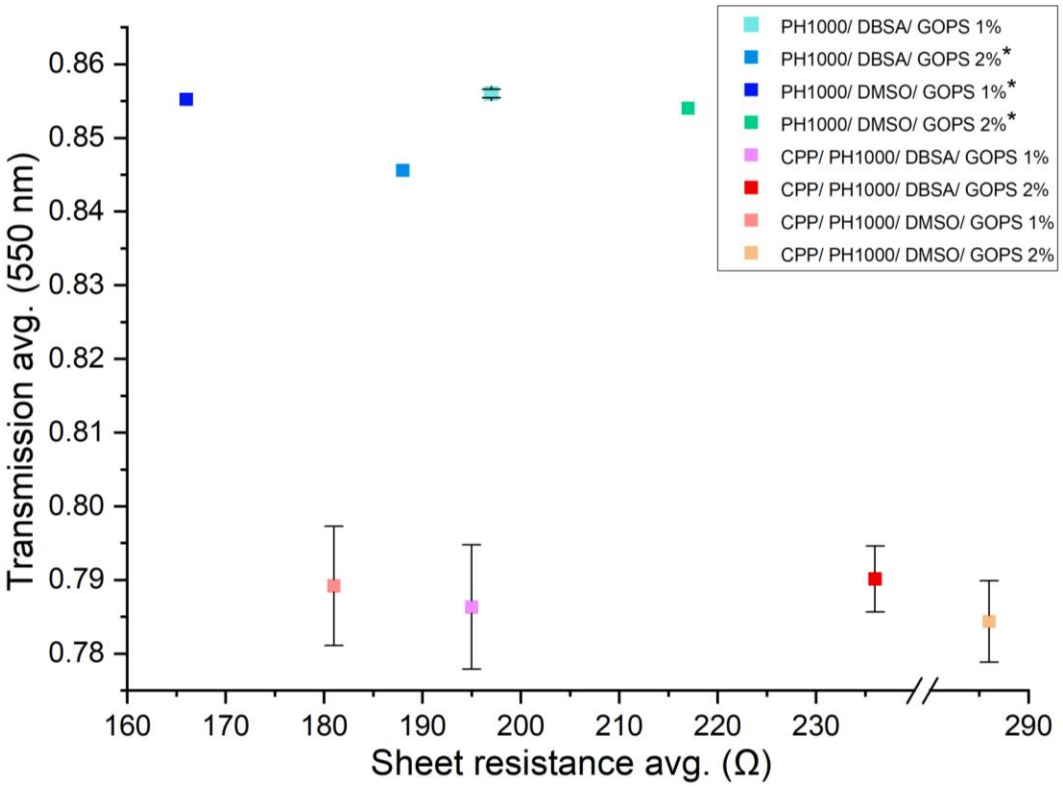

Figure 12. average sheet resistance vs average transmission (at 550 nm) for the different sample groups

Based on Figure 12 a few estimations can be made on the conductivity of the individual glass films. The most favorable result for the samples would be a low sheet resistance and a high transmission as can be seen for the PH1000/ DMSO/ GOPS 1% group. In contrast, samples such as CPP/ PH1000/ DMSO/ GOPS 2% with a high sheet resistance and low transmission can be estimated to have a low conductivity and thus are the least ideal film. There seem to be no strong divides between sample groups which contain either DBSA or DMSO but the highest contrast for both transmission and sheet resistance results arises from the GOPS concentration with the GOPS 2% scoring overall lower results.

The influence of the double layers with the CPP is also made more clearly in Figure 12. While the sheet resistance of CPP/ PH1000/ DBSA/ GOPS 1% and its equivalent additive DMSO group seem to be within the same range as PH1000/ DBSA/ GOPS 1%, the transmission is far lower than that of single layer samples. This is a direct result of the double layered film being thicker and thus less transparent as both CPP and PH1000 solutions have a light blue hue when coated.

The film thickness was lastly measured to conclude the analysis of the glass samples, and the average conductivity was calculated for the sample groups as can be seen in Table 7.

Table 7. Average conductivity and film thickness of the double- and single-layer sample groups and the St.deviation

Coating	Avg. conductivity (S/cm)	St.dev (+/-)	Avg. film thickness (nm)	St.dev (+/-)
PH1000/ DBSA/ GOPS 1%	355	124	165	21
PH1000/ DBSA/ GOPS 2% *	421	/	126	/
CPP/ PH1000/ DBSA/ GOPS 1%	82	15	583	59
CPP/ PH1000/ DBSA/ GOPS 2%	66	16	585	66
PH1000/ DMSO/ GOPS 1% *	442	/	135	/
PH1000/ DMSO/ GOPS 2% *	232	/	198	/
CPP/ PH1000/ DMSO/ GOPS 1%	123	13	546	21
CPP/ PH1000/ DMSO/ GOPS 2%	58	21	585	23

A single layered CPP film thickness was additionally measured to test for the individual thickness of the CPP without the PH1000 layer. On average the CPP layer thickness would be 530 nm while single PH1000 layers would range between 126 – 198 nm. The most significant difference in conductivity and film thickness is between double layers of CPP/ PH1000 and single layers PH1000.

Since solutions with GOPS 2% had a highly fluctuating sheet resistance and conductivity, the values presented in Table 7 cannot be considered a standard of such films. The most stable and conductive films were PH1000/ DBSA/ GOPS 1% and PH1000/ DMSO/ GOPS 1%. A comparison between the two groups shows that the PH1000/ DMSO/ GOPS 1% had overall a better conductivity, transmission, and a thinner film thickness even though the coating settings were the same for all samples. The thicker film for samples containing DBSA can be attributed to the high viscosity of the DBSA additive.

4.2.2 Cyclic voltammetry of ITO samples (PTFE)

The cyclic voltammetry experiments were not performed for all sample groups since the results from the first few experiments have shown that the PTFE filter caused fundamental changes to the structure of the PEDOT:PSS solution which were undesirable.

The most apparent difference between samples using PTFE filters and samples using RC filters was the standard color change of the PH1000 layer, which is visible when PEDOT oxidizes

during CV. This color change was not observable for the PH1000 solutions which were filtered with PTFE. The first sample which was tested was PH1000/ DMSO/ GOPS 1% since the conductivity experiments showed that this sample group was the most promising one when compared to other films. A standard scan rate of 50 mV/s was used, and the cycles were running between 0.8 V and -1 V. During the experiment no color change was optically seen nor did the potentiostat measure any oxidation or reduction peaks as expected from the PEDOT molecule. Furthermore, the CV for the tested sample showed a severe lack in electrical capacitance.

To confirm that this occurrence was not exclusive for the PH1000/ DMSO/ GOPS 1% group, additional testing was done with PH1000/ DMSO/ GOPS 2% samples with the same settings as previously. The experiments yielded similar results and can be seen in Figure 13 where a comparative CV graph of the same PH1000/ DMSO/ GOPS 2% solution filtered via RC can be seen. The RC filtered sample shows a higher capacitance and discernible oxidation and reduction peaks.

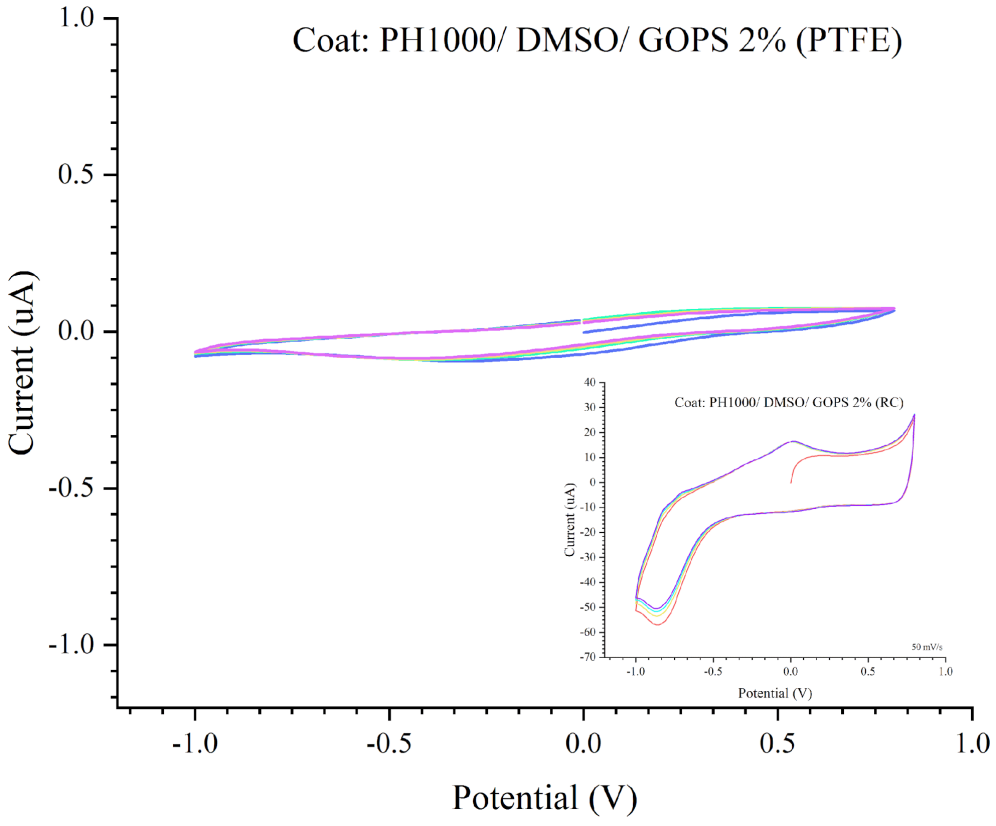

Figure 13. CV of PH1000/ DMSO/ GOPS 2% (PTFE) sample with no oxidation peaks compared to PH1000/ DMSO/ GOPS 2% (RC) in the bottom right corner

None of the samples which were tested afterwards showed any improvement thus the CV experiments were cut short for PH1000 solutions filtered with PTFE.

The exact effect that the PTFE filter had on the PEDOT:PSS structure is unclear, but a few theories based on the information obtained from these experiments can be constructed.
As described in "Growth Mechanism of Strain-Dependent Morphological Change in PEDOT:PSS Films", the PEDOT:PSS morphology is made of conductive, tangled PEDOT-rich cores which are surrounded by PSS chains (see section 1.1). [30] When the PH1000 solution was filtered through the hydrophobic PTFE, the hydrophilic PEDOT-rich cores would have the most difficulty passing through. This was a noticeable effect since at the beginning of the filtration, the resistance offered by the filter was minimal but the more PH1000 solution was being pushed through, the more force needed to be applied as the resistance increased. Thus, it can be theorized that with an increase in filtered solution there was also an increase in the aggregation of rich PEDOT-cores on the surface of the filter which resulted in the filter becoming congested. With sufficient force the PEDOT:PSS solution could be pushed through, but the most likely outcome was a stark change in the morphology if not also a disruption in the bonds between the PEDOT and PSS.

What can be concluded is that filtering a PEDOT:PSS solution through a PTFE filter will cause changes most probably in both morphology and structure. Considering that there are samples such as PH1000/ DMSO/ GOPS 1% which are very conductive it could be concluded that bonds which might be disrupted during filtration can reconstruct afterwards to a certain extent.
A permanent change produced by the filter which is irreversible is most likely caused to the morphology of PEDOT:PSS since both the surface tension and electrical capacitance show a strong change and thus there is possibly a lack of PEDOT-rich cores within the solution.

4.3 RC filtered solutions

The samples which were produced with PH1000 solutions filtered by RC no longer contained DBSA. Since the experiments with PTFE have shown no significant difference between the conductivity of PH1000 containing DBSA or DMSO it was determined that the DMSO additive was better due to its low viscosity and thus easier use of pipetting. While there were many problems with applying the PH1000 solutions filtered by RC to glass and ITO, the electrical capacitance was far better when compared to the PTFE results.

Establishing a standard for the conductivity of the RC filtered PH1000 solutions was difficult since an even coating is necessary for an accurate van-der Pauw measurement and many of the samples had less than ideal films. The single layered PH1000 films often contained uncoated edges or porous layers which would strongly affect the sheet resistance and conductivity results. There was one result for a single layer PH1000 coating which far exceeded the other samples in terms of coating integrity and conductivity. This was due to a change in the appliance method of the substrate to glass during spin coating. This sample, which will be denoted here as PH1000/ DMSO/ GOPS 1% (double), was produced by first applying the PH1000 solution and spin-coating it on glass as described in section 3.3. After the spin-coater was done, the PH1000/ DMSO/ GOPS 1% solution was applied a second time on the fresh film and left to rest for a few seconds before the spin-coater was started again with the same settings. The film was then annealed, and the exact results can be seen in section 4.2.1.

4.3.1 Conductivity of glass samples (RC)

While the overall results for the sheet resistance had less deviations, the film of the glass samples for single layered PH1000 samples was oftentimes not completely covering the entire area of the glass due to the solutions lack of adhesion and high surface tension. The double layers were thus more useful since the CPP coat offered the required support for the PH1000 solution to create an even film. Additionally, the RC filter kept the PEDOT:PSS structure intact allowing for a high sample conductivity despite the double layer. The average sheet resistance for the sample groups as well as the sample PH1000/ DMSO/ GOPS 1% (double) can be seen in Table 8.

Table 8. Average sheet resistance of single layer and double layers with additive DMSO and GOPS 1 or 2 % and the sample PH1000/ DMSO/ GOPS 1% (double), used sample number and standard deviation

Coating	**Sample Nr**	**Avg. sheet resistance (Ω)**	**St. dev (+/-)**
PH1000/ DMSO/ GOPS 1%	2	211	8
PH1000/ DMSO/ GOPS 2%	2	251	21
PH1000/ DMSO/ GOPS 1% (double)	1	239	/
CPP/ PH1000/ DMSO/ GOPS 1%	2	177	5
CPP/ PH1000/ DMSO/ GOPS 2%	2	236	1,4

The high deviation for the sample group PH1000/ DMSO/ GOPS 2% was a result of the difficult coating process that would be present for all single layered PH1000 samples, but the GOPS 2% made it more challenging. While there were no measurements taken for the surface tension of PH1000/ DMSO/ GOPS 1% and PH1000/ DMSO/ GOSP 2%, there were noticeable appliance differences between the two sample groups. When the solution was applied to the glass or ITO sample as described in section 3.3.3, the droplets would merge and pull away from the area they were applied to more vigorously than PH1000 solutions with GOPS 1%. This was an indication that the PH1000/ DMSO/ GOPS 2% would adhere to itself more than to the glass or ITO surface, making the coating more unpredictable and more prone to failure.

For the RC filtered solutions it was difficult to discern any notable differences between the different coatings even when a sheet resistance vs transmission graph was established. Thus, the film thickness was measured, and a conductivity vs transmission (550 nm) graph was made to better compare the different samples (see Figure 14).

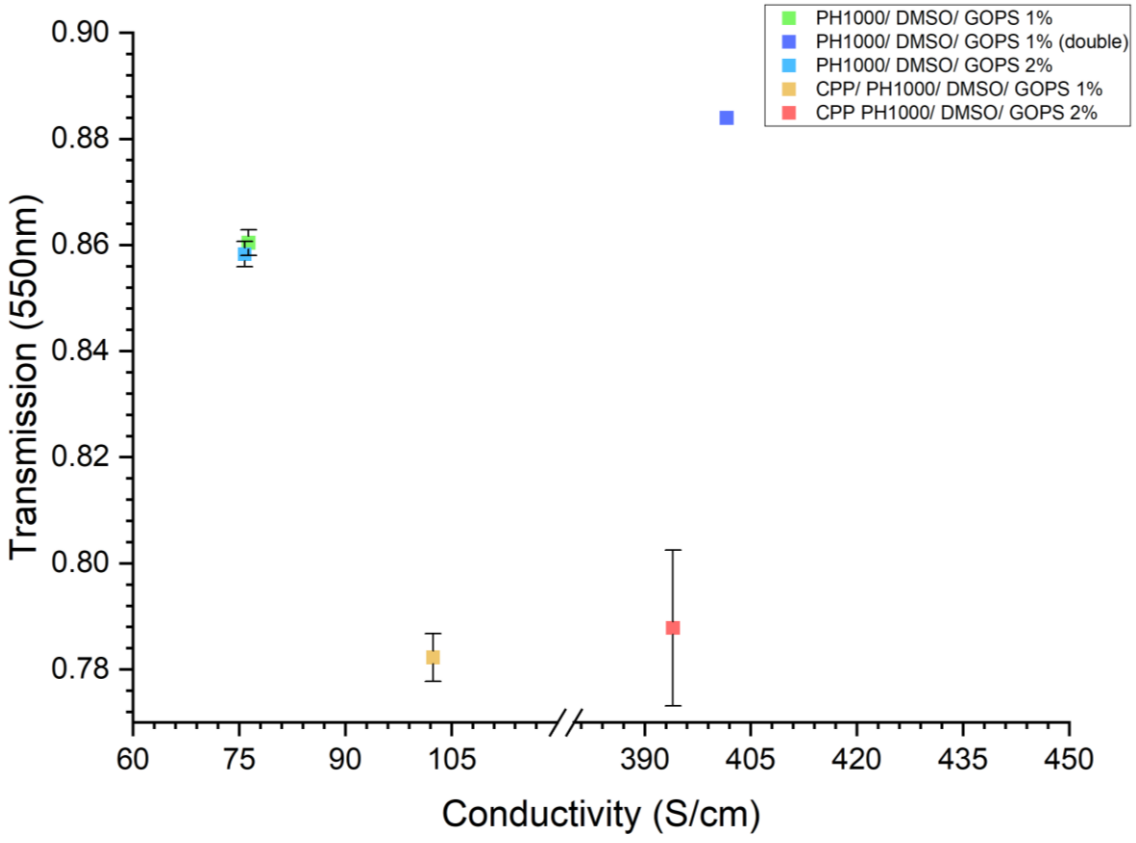

Figure 14. Conductivity vs transmission (550 nm) of different sample group averages and the sample PH1000/ DMSO/ GOPS 1% (double)

As previously described, samples containing a CPP layer have a lowered transmission which is due to the double layers' decrease in transparency. The single film PH1000 samples have a far lower conductivity due to an irregular coating which leaves gaps throughout the film and thus decreasing conductivity.

Furthermore, the sample PH1000/ DMSO/ GOPS 1% (double) has the highest transmission and conductivity from all tested sample groups. This is a direct result of the different appliance method used for this individual sample. Considering that the method was only tested once on the PH1000/ DMSO/ GOPS 1% (double) sample it is not clear whether the change in the spin-coating process would yield a consistently improved film. Since the sheet resistance of the sample did not show any significant difference when compared to the other samples, it can be concluded that the increase of the transmission stems from the decrease in film thickness which can be seen in Table 9. The reason behind the stark increase in conductivity is unclear or the sample measurements could be erroneous.

Table 9. Conductivity and film thickness of PH1000/ DMSO/ GOPS 1% (double) and the averages of the different sample groups

Coating	**Avg. conductivity (S/cm)**	**St.dev (+/-)**	**Avg. film thickness (nm)**	**St.dev (+/-)**
PH1000/ DMSO/ GOPS 1%	76	7	119	8×10^{-1}
PH1000/ DMSO/ GOPS 1% (double)	401	/	104	/
PH1000/ DMSO/ GOPS 2%	75	2	150	4
CPP/ PH1000/ DMSO/ GOPS 1%	102	2	531	6
CPP/ PH1000/ DMSO/ GOPS 2%	394	17	575	21

For the sample PH1000/ DMSO/ GOPS 1% (double) the film thickness could fluctuate between 95 nm and 108 nm depending on whether the measurement was taken at the center of the sample or towards the edge. Most single layer PH1000 samples had an average layer thickness of 120-190 nm depending on whether the solution contained 1 or 2% GOPS. Samples with GOPS 1% had a tendentially smaller film thickness than samples with GOPS 2%.

4.3.2 Cyclic voltammetry of ITO coated (RC)

The electrical capacitance experiments for RC filtered PH1000 solutions were performed for single layered PH1000 films and double layered CPP/ PH1000 films. Additionally, single layered CPP (slow) and CPP (fast) samples were also analyzed to better compare the effect of the layer thickness of CPP on the overall electrical capacitance of double layered electrodes. As described in section 3.3.3, an area of 10 x 30 mm was spin-coated but due to the appliance difficulties of single layered PH1000 solutions the CV tested area for such samples varied. The exact area size which was analyzed during CV was measured by oxidizing the ITO after the experiment was completed and manually measuring the discolored area of the ITO. First the CPP (slow) and CPP (fast) were tested, and the results can be seen in Figure 15.

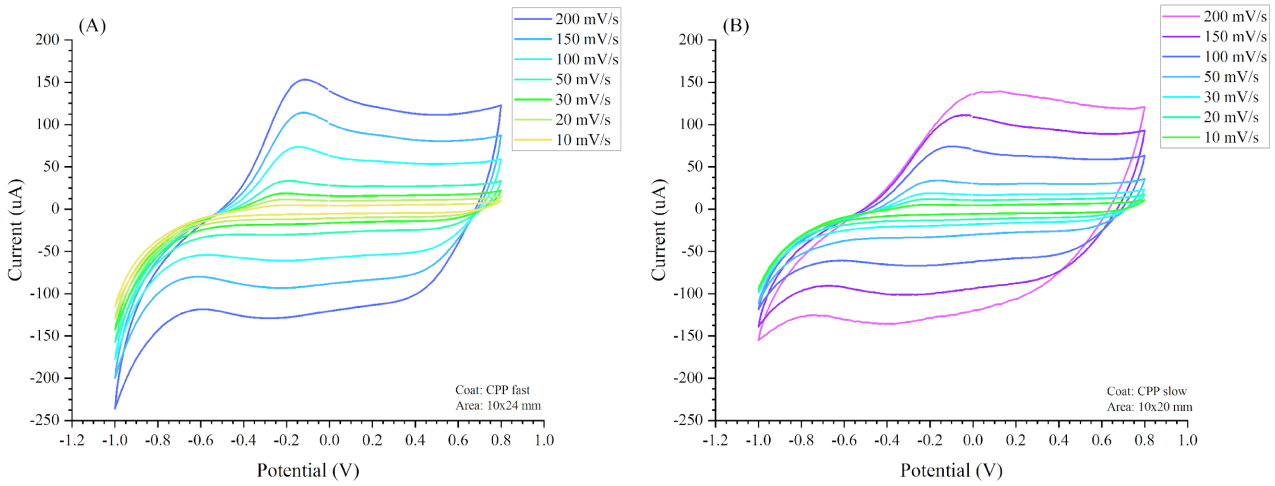

Figure 15. Left graph (A) of CPP (fast) shows a higher electrical capacitance with the highest peak reaching 153 µA than the right graph (B) of CPP (slow) with the highest peak at 138 µA. The area of the CPP (slow) sample is 4 mm smaller than that of the CPP (fast) sample.

The difference in electrical capacitance is not exceedingly high between the CPP (fast) and CPP (slow) coating, but the CPP (fast) has a slightly higher current range than CPP (slow). By using the CV graph and the area size of the individual samples the volumetric capacitance was calculated as described in the following formula:

$$C_v = \frac{\int j dV}{2v(V_{max} - V_{min})I_d} \qquad \text{(eq. 4)}$$

C_v … volumetric capacitance

j … current density

v … scan rate

ΔV … potential window

I_d … sheet thickness

The following values for volumetric capacitance were obtained at different scan rates.

Table 10. Calculated volumetric capacitance for samples CPP (fast) and CPP (slow)

	CPP (fast)	**CPP (slow)**
Scan rate (mV s^{-1})	Capacitance (F cm^{-3})	Capacitance (F cm^{-3})
200	5.07	4.73
150	5.02	4.96
100	5.33	5.17
50	3.86	6.12
30	7.96	6.95
20	9.41	8.15
10	14.16	12.19

As can be seen in Table 10. The difference in volumetric capacitance between the two samples is not very significant. While CPP (fast) has a slightly higher capacitance it also has an unusual drop at the 50 mV s^{-2} scan rate.

It can be concluded, that the difference in volumetric capacitance between CPP coatings of different sheet thicknesses is insignificant with the tested spin coating speeds.

The next samples which were tested were single layered PH1000 coatings and the results can be seen in Figure 16.

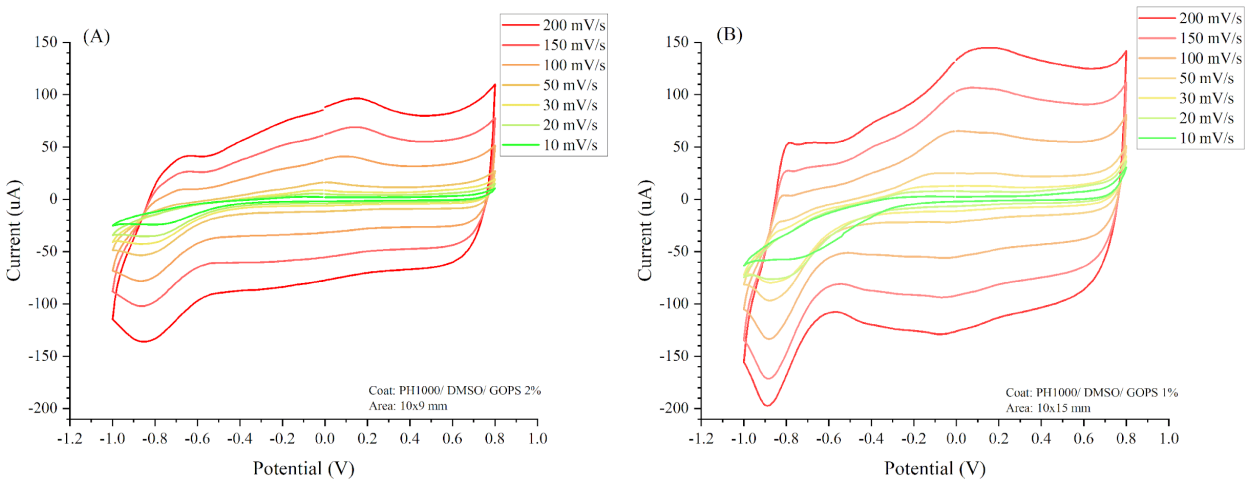

Figure 16. Left graph (A) depicts the CV of the PH1000/ DMSO/ GOPS 2% and the right graph (B) of PH1000/ DMSO/ GOPS 1%. The tested area in (A) is 10 x 9 mm and thus 6 mm smaller in length than the area of (B)

The area discrepancy between the two single layered PH1000 samples makes it more difficult to get a direct comparison of the electrical capacitance, but the CV graph in (B) of Figure 16 shows that the oxidation and reduction peaks are much more pronounced than in graph (A). This could be due to the different GOPS concentrations or the smaller area which was analyzed. The exact capacitance which can be seen in Table 11 shows that the PH1000/ DMSO/ GOPS 1% sample had a similar starting capacitance as PH1000/ DMSO/ GOPS 2% but grew larger at lower scan rates than its counterpart.

Table 11. Calculated capacitance for samples PH1000/ DMSO/ GOPS 2% and PH1000 / DMSO/ GOPS 1%

	PH1000/ DMSO/ GOPS 2%	**PH1000/ DMSO/ GOPS 1%**
Scan rate (mV s^{-1})	Capacitance (F cm^{-3})	Capacitance (F cm^{-3})
200	28.15	30.46
150	26.42	30.50
100	24.26	28.95
50	22.89	29.65
30	20.93	36.73
20	31.94	50.77
10	43.33	83.11

Since it was easier to spin-coat both PH1000/ DMSO/ GOPS 1% and 2% on CPP, double layered samples were also tested with CV to get a better comparison of the electrical capacitance which can be seen in Figure 17.

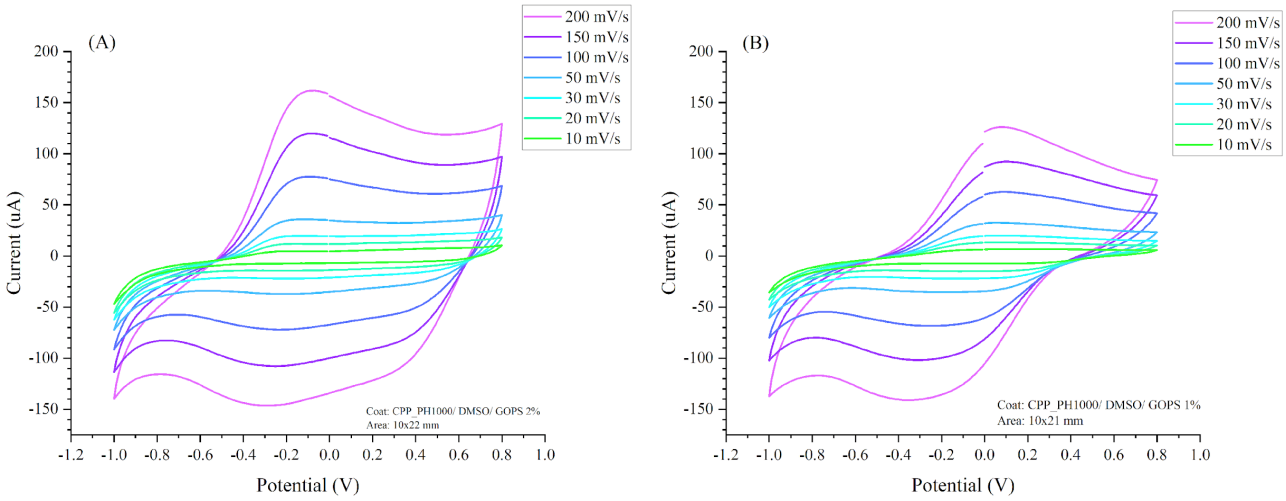

Figure 17. CV of double layered CPP/ PH1000/ DMSO/ GOPS 2% (A) and CPP/ PH1000/ DMSO/ GOPS 1% (B) with an equal area size.

The CPP/ PH1000/ DMSO/ GOPS 2% has larger and broader areas as well as a higher maximum peak reaching 161 µA. The equivalent GOPS 1% sample has more defined oxidation and reduction areas which are overall smaller and has a maximum current peak of 126 µA. In both experiments the oxidation peaks of the PEDOT:PSS structure were shifted from -0.8 V (see Figure 17) to approximately -0.3 V. The evaluated volumetric capacitance can be seen in Table 12.

Table 12. Calculated capacitance for samples PH1000/ DMSO/ GOPS 2% and PH1000 / DMSO/ GOPS 1%

	CPP/ PH1000/ DMSO/ GOPS 2%	**CPP/ PH1000/ DMSO/ GOPS 1%**
Scan rate (mV s^{-1})	Capacitance (F cm^{-3})	Capacitance (F cm^{-3})
200	4.15	3.51
150	4.12	3.45
100	4.24	3.68
50	4,81	4.34
30	5.28	4.95
20	5.62	5.47
10	6.96	7.01

While it was more challenging to compare the single layered samples, the double layered CV analysis shows that the capacitance for the sample containing GOPS 2% is approximately equal to that of the GOPS 1% sample.

4.4 Comparing PTFE filter vs RC filter results

Both PTFE and RC results have shown improvements and deteriorations in opposing areas. The PTFE solutions were much easier to coat without the additional support from a CPP layer, but the conductivity was inconsistent, and the electrical capacity was barely present. The RC solutions rarely produced complete coatings without the underlying CPP film but when the PH1000 films were ideal, the conductivity and electrical capacitance were much better than previous samples. The difference between DBSA and DMSO was non-significant while the GOPS concentration caused a lot of behavior changes in the PH1000 solutions. In order to understand how the appliance, conductivity, and electrical capacity of the PEDOT:PSS solutions were changed due to the GOPS concentration and the filters, the PTFE results must be analyzed more closely.

The definitive information which can be drawn from the PTFE filtration is that PEDOT was being filtered from the PH1000 solution randomly. This can be concluded from the highly varying conductivity results from the PTFE samples in comparison to the RC groups. In order for the PEDOT:PSS film to be conductive, it requires the presence of PEDOT within the structure. Thus, the PTFE filter which removes hydrophilic components such as PEDOT would do so at random rates since a lot of force was applied during the filtration to press as much of the PH1000 solution through the filter as possible. This would allow for a random amount of PEDOT to always be present in the PH1000 solution. Furthermore, if the varied PEDOT amount causes fluctuating conductivity results, then the same randomness should be observable for the electrical capacitance experiments of PTFE samples if the electrical capacitance is solely dependable on the oxidation and reduction of PEDOT. These varying results were not observable for the CV experiments as all results have barely shown any electrical capacitance and no variety in oxidation and reduction peaks. This would lead to the conclusion that the electrical capacitance is dependable on the morphology of the PEDOT:PSS structure.
PEDOT-rich cores are less likely to pass through the filter than PEDOT bound to PSS rich areas thus the standard morphology for PEDOT:PSS would be lost through the PTFE filtration. This

would lead to the results which are present in these experiments, since the random amount of PEDOT within PSS rich areas would allow for varying conductivity results but the complete loss of PEDOT-rich cores would give no electrical capacitance results.

Furthermore, it is not just the electrical capacitance which is dependable on the PEDOT:PSS morphology. From the different additives that were used in the PH1000 solution, the GOPS concentration, which improves water-stability and crosslinks the structure of PEDOT:PSS, created significant effects to the results in all tested areas. For RC filtered samples, the higher GOPS concentration (2%) made application of single layered PH1000 more challenging than the PH1000/ DMSO/ GOPS 1% which was slightly more successful. Additionally for RC tested samples, when an equally complete PH1000 coating was created on top of a CPP layer the electrical capacitance was equal for PH1000 films which contained GOPS 2% and GOPS 1%. The CPP/ PH1000/ DMSO/ GOPS 2% had a conductivity of 394 (S/cm) and a larger current range than its counterpart group. The RC filter samples which had one PH1000 layer had similar electrical capacitance when compared to other literature values which reached 39 F/ cm^3. [31]. Since the cleaning process of all samples was done manually, it is possible that unwanted remnants were still on the surface of the glass/ ITO which could be the cause of differing results. This could also have influenced the coating process and showcase how a sonicated bath is necessary for spin coating PH1000 on different substrates. Another possibility for the appliance difficulty of solutions containing GOPS 2% is speculated to be due to the increased surface tension which would also indicate a stronger interaction of intermolecular forces thus further supporting the idea that the morphology of PEDOT:PSS has a significant effect in all analyzed areas.

A stronger, more dense morphological structure of PEDOT-rich cores leads to stronger intermolecular interactions creating a better conductivity and electrical capacitance in ideal films and decreasing overall appliance without CPP layer support. The opposite effect of decreasing and weakening the PEDOT-rich cores leads to better appliance of PH1000 as a single layered coating but decreases conductivity and electrical capacitance as seen from the PTFE results.

The previously mentioned delamination issues were not observable for any samples produced during these experiments.

5. Conclusion

The cyclic voltammetry of ITO shows that a potential of more than -1.1 V will cause a reduction during the negative sweep and an oxidation at -0.8 V during the positive sweep. Thus, the operational window for electrodes spin coated on ITO glass with a HEPES electrolyte, was determined to be between 0.8 V and -1 V at a pH of 7.4.
A possible reduction of oxygen was determined to be at approximately -1.4 V since the reduction curve did not appear on the cyclic voltammetry under nitrogen conditions. Furthermore, it could be theorized that the reduction of ITO yields various oxidation states of In which then react to In_2O_3 during the positive sweep. Additionally, In^0 is also speculated to be produced on the ITO surface during the negative sweep, causing a metallic ochre layer to form on the surface of the glass.

ITO and glass samples which were spin coated with PTFE filtered solutions have shown an improvement in appliance and a decrease in conductivity and electrical capacitance. This result is theorized to be due to the filtration of the hydrophilic PEDOT-cores in the PH1000 solutions via the hydrophobic PTFE filter which had a visible decrease in the surface tension of the solution. Some PEDOT would still be present in PSS-rich areas which resulted in a high variety of conductivity results but an overall low electrical capacitance and no reaction peaks of PEDOT during cyclic voltammetry experiments. This led to the conclusion that PEDOT-cores played an important role in the PEDOT-PSS compound and are clearly necessary for the electrical capacitance and oxidation and reduction reaction of PEDOT.

Further analysis using RC filters with PH1000 solutions have shown a decrease in appliance but an overall increase in conductivity and electrical capacitance when compared to the PTFE results. The best result for conductivity was achieved by the sample PH1000/ DMSO/ GOPS 1% (double) which was spin-coated twice before annealing. Since the solution was additionally applied twice, it allowed for a better layer coverage and a thinner film while the resistance was equal to other single layered PH1000 samples.

All other single layered PH1000 samples had a good transmission but the conductivity was lacking due to the poor adhesion of the solution to the glass. This issue could be solved by using a supporting CPP layer which decreased the transmission but improved overall appliance of the PH1000 solution and thus improving conductivity.

The CV for RC filtered samples have given poor results when compared to literature values, which is speculated to be due to the cleaning process of the ITO glass. Since the cleaning process was performed manually, residual components could still be on the surface of the glass and thus interfering with the ITO and PH1000 layer connectivity. This could further explain the issues which were encountered during the appliance process of the PH1000 solution on ITO and glass. The PH1000 solution was more difficult to spin coat the higher the GOPS concentration was even though the additive had an intended effect of improving appliance. [17]

While the electrical capacitance between the double layered samples had no significant differences, the result of the PH1000/ DMSO/ GOPS 1% was slightly better than its counterpart.

There were no layer delamination issues observable during any experiments which were performed with glass or ITO.

6. References

1. Shintani, Kelly, et al. “Review and Update: Current Treatment Trends for Patients With Retinitis Pigmentosa.” *Optometry - Journal of the American Optometric Association*, vol. 80, no. 7, Elsevier BV, July 2009, pp. 384–401. https://doi.org/10.1016/j.optm.2008.01.026.

2. Fahim, Abigail. “Retinitis Pigmentosa.” *Current Opinion in Pediatrics*, vol. 30, no. 6, Ovid Technologies (Wolters Kluwer Health), Dec. 2018, pp. 725–33. https://doi.org/10.1097/mop.0000000000000690.

3. Curcio, Christine A., and Kimberly A. Allen. “Topography of Ganglion Cells in Human Retina.” The Journal of Comparative Neurology, vol. 300, no. 1, Wiley, Oct. 1990, pp. 5–25. https://doi.org/10.1002/cne.903000103.

4. Dacey, D. “Primate Retina: Cell Types, Circuits and Color Opponency.” *Progress in Retinal and Eye Research*, vol. 18, no. 6, Elsevier BV, Nov. 1999, pp. 737–63. https://doi.org/10.1016/s1350-9462(98)00013-5.

5. Fain, Gordon L., et al. “Phototransduction and the Evolution of Photoreceptors.” *Current Biology*, vol. 20, no. 3, Elsevier BV, Feb. 2010, pp. R114–24. https://doi.org/10.1016/j.cub.2009.12.006

6. Gray-Keller, Mark P., and Peter B. Detwiler. “The Calcium Feedback Signal in the Phototransduction Cascade of Vertebrate Rods.” *Neuron*, vol. 13, no. 4, Elsevier BV, Oct. 1994, pp. 849–61. https://doi.org/10.1016/0896-6273(94)90251-8.

7. Alloway, Kevin D. “*Neuroscience*. Dale Purves , George J. Augustine , David Fitzpatrick , Lawrence C. Katz , Anthony-Samuel LaMantia , James O. McNamara , S. Mark Williams.” *The Quarterly Review of Biology*, vol. 76, no. 4, University of Chicago Press,

Dec. 2001, pp. 526–526. https://doi.org/10.1086/420640.

8. Hamel, Christian. “Retinitis Pigmentosa.” *Orphanet Journal of Rare Diseases*, vol. 1, no. 1, Springer Science and Business Media LLC, Oct. 2006, https://doi.org/10.1186/1750-1172-1-40.

9. Pagon, Roberta A. “Retinitis Pigmentosa.” *Survey of Ophthalmology*, vol. 33, no. 3, Elsevier BV, Nov. 1988, pp. 137–77. https://doi.org/10.1016/0039-6257(88)90085-9.

10. Narayan, Daniel S., et al. “A Review of the Mechanisms of Cone Degeneration in Retinitis Pigmentosa.” *Acta Ophthalmologica*, vol. 94, no. 8, Wiley, June 2016, pp. 748–54. https://doi.org/10.1111/aos.13141.

11. Groenendaal, L., et al. “Poly(3,4-ethylenedioxythiophene) and Its Derivatives: Past, Present, and Future.” *Advanced Materials*, vol. 12, no. 7, Wiley-Blackwell, Apr. 2000, pp. 481–94. https://doi.org/10.1002/(sici)1521-4095(200004)12:7.

12. Sun, Kuan, et al. “Review on Application of PEDOTs and PEDOT:PSS in Energy Conversion and Storage Devices.” *Journal of Materials Science: Materials in Electronics*, vol. 26, no. 7, Springer Science and Business Media LLC, Mar. 2015, pp. 4438–62. https://doi.org/10.1007/s10854-015-2895-5.

13. Yoo, Dohyuk, et al. “Direct Synthesis of Highly Conductive Poly(3,4-ethylenedioxythiophene):Poly(4-styrenesulfonate) (PEDOT:PSS)/Graphene Composites and Their Applications in Energy Harvesting Systems.” *Nano Research*, vol. 7, no. 5, Springer Science and Business Media LLC, Apr. 2014, pp. 717–30. https://doi.org/10.1007/s12274-014-0433-z.

14. Wen, Yangping, and Jingkun Xu. “Scientific Importance of Water-Processable PEDOT-PSS and Preparation, Challenge and New Application in Sensors of Its Film Electrode: A Review.” *Journal of Polymer Science Part A: Polymer Chemistry*, vol. 55, no. 7, Wiley,

Feb. 2017, pp. 1121–50. https://doi.org/10.1002/pola.28482.

15. Bengtssom et al. “Conducting Polymer Electrodes for Gel Electrophoresis.” *PloS ONE*, edited by Alexei Gruverman, vol. 9, no. 2, Public Library of Science (PloS), Feb. 2014, p. e89416. https://doi.org/10.1371/journal.pone.0089416.

16. Wang, Zifei, et al. “Facile Preparation of Highly Water-stable and Flexible PEDOT:PSS Organic/Inorganic Composite Materials and Their Application in Electrochemical Sensors.” *Sensors and Actuators B: Chemical*, vol. 196, Elsevier BV, June 2014, pp. 357–69. https://doi.org/10.1016/j.snb.2014.02.035.

17. Håkansson, Anna, et al. “Effect of (3-glycidyloxypropyl)Trimethoxysilane (GOPS) on the Electrical Properties of PEDOT:PSS Films.” *Journal of Polymer Science Part B: Polymer Physics*, vol. 55, no. 10, Wiley, Mar. 2017, pp. 814–20. https://doi.org/10.1002/polb.24331.

18. Piro, Benoît, et al. “Fabrication and Use of Organic Electrochemical Transistors for Sensing of Metabolites in Aqueous Media.” *Applied Sciences*, vol. 8, no. 6, MDPI AG, June 2018, p. 928. https://doi.org/10.3390/app8060928.

19. Lin, Yow-Jon, et al. “Changing Electrical Properties of PEDOT:PSS by Incorporating With Dimethyl Sulfoxide.” *Chemical Physics Letters*, vol. 664, Elsevier BV, Nov. 2016, pp. 213–18. https://doi.org/10.1016/j.cplett.2016.10.038.

20. Ma, Zhizhen, et al. “Indium-Tin-Oxide for High-performance Electro-optic Modulation.” *Nanophotonics*, vol. 4, no. 1, Walter de Gruyter GmbH, June 2015, pp. 198–213. https://doi.org/10.1515/nanoph-2015-0006.

21. Lingstedt, Leona V., et al. “Effect of DMSO Solvent Treatments on the Performance of PEDOT:PSS Based Organic Electrochemical Transistors.” *Advanced Electronic*

Materials, Wiley, Feb. 2019, p. 1800804. https://doi.org/10.1002/aelm.201800804.

22. Zhang, Yuantao, et al. "Gas-sensing Properties of ITO Materials With Different Morphologies Prepared by Sputtering." *SN Applied Sciences*, vol. 2, no. 2, Springer Science and Business Media LLC, Jan. 2020, https://doi.org/10.1007/s42452-020-2050-7.

23. Ho, S. M. "A Review on Thin Films on Indium Tin Oxide Coated Glass Substrate." *Asian Journal of Chemistry*, vol. 28, no. 3, Asian Journal of Chemistry, 2016, pp. 469–72. https://doi.org/10.14233/ajchem.2016.19579.

24. Minami, Tadatsugu. "Present Status of Transparent Conducting Oxide Thin-film Development for Indium-Tin-Oxide (ITO) Substitutes." *Thin Solid Films*, vol. 516, no. 17, Elsevier BV, July 2008, pp. 5822–28. https://doi.org/10.1016/j.tsf.2007.10.063.

25. Arvidsson, Rickard, et al. "Energy and Resource Use Assessment of Graphene as a Substitute for Indium Tin Oxide in Transparent Electrodes." *Journal of Cleaner Production*, vol. 132, Elsevier BV, Sept. 2016, pp. 289–97. https://doi.org/10.1016/j.jclepro.2015.04.076.

26. Ouyang, Jianyong. "Solution-Processed PEDOT:PSS Films With Conductivities as Indium Tin Oxide Through a Treatment With Mild and Weak Organic Acids." *ACS Applied Materials &Amp; Interfaces*, vol. 5, no. 24, American Chemical Society (ACS), Dec. 2013, pp. 13082–88. https://doi.org/10.1021/am404113n.

27. Yang, Hongsheng, et al. "Indium Tin Oxide-free Polymer Solar Cells Using a PEDOT : PSS/Ag/PEDOT : PSS Multilayer as a Transparent Anode." *Journal of Physics D: Applied Physics*, vol. 45, no. 42, IOP Publishing, Oct. 2012, p. 425102. https://doi.org/10.1088/0022-3727/45/42/425102.

28. Erdene-Ochir, Otgonbayar. *Investigation of Polymer Electrode – Electrolyte Interfaces for Future Neurostimulating Photosensors*. University of Cologne, 2021.

29. van der Pauw Measurement using Keithley 2400 and LabTracer n.d., last accessed on 19 December 2022, https://engineering.purdue.edu/Powerlab/Standard%20Operating%20Procedures/vFinal%20van%20der%20Pauw%20Testing%20User%20Guide%20%202014.pdf

30. Lee, Yoo-Yong, et al. "Growth Mechanism of Strain-Dependent Morphological Change in PEDOT:PSS Films." *Scientific Reports*, vol. 6, no. 1, Springer Science and Business Media LLC, Apr. 2016, https://doi.org/10.1038/srep25332.

31. Jonathan Rivnay et al. "High-performance transistors for bioelectronics through tuning of channel thickness", *Science Advances*, 2015.